

On the importance of frequency-dependent beam parameters for vacuum acceleration with few-cycle radially-polarized laser beams

Spencer W. Jolly*

LIDYL, CEA, CNRS, Université Paris-Saclay, CEA Saclay, 91 191 Gif-sur-Yvette, France

(Dated: February 1, 2022)

Tightly-focused, ultrashort radially-polarized laser beams have a large longitudinal field, which provides a strong motivation for direct particle acceleration and manipulation in vacuum. The broadband nature of these beams means that chromatic properties of propagation and focusing are important to consider. We show via single particle simulations that using the correct frequency-dependent beam parameters is imperative, especially as the pulse duration decreases to the few-cycle regime. The results with different spatio-spectral amplitude profiles show both a drastic increase or decrease of the final accelerated electron energy depending on the shape, motivating both proper characterization and potentially a route to optimization.

The longitudinal acceleration of electrons with high-power tightly-focused radially-polarized laser beams (RPLBs) is a promising method for particle acceleration in vacuum and provides a rich platform for studying relativistic particle dynamics and the proper modeling of the focused fields [1–3]. Simulations to date have progressed to use representations for the field that are accurate non-paraxially to high order [4–8] and have even included inter-particle interactions and radiation reaction models [9]. Experimental results have been impressive [10, 11], but still require an enhanced knowledge of the complete field to understand the limitations and to predict future results. Recent attempts have been made to show the effect of chromatic focusing and linear chirp [12], and the potential of a large number of other aberrations are so far unexplored. However, these simulations have all so far not considered the amplitude and phase effects that become important in the diffraction of very short pulses approaching the few-cycle regime [13–16]. This manuscript will simulate the effect of the frequency-dependent beam parameters on acceleration with few-cycle RPLBs, showing a significant effect. This has been explored for a single case of sub-cycle and single-cycle pulses [17, 18], where we show rather the effect for various designed spatio-spectral profiles at many laser powers and pulse durations.

Diffraction effects become significant in the few-cycle regime for a very simple reason, because diffraction—the crucial mechanism to model when tightly focusing any laser beam—is itself chromatic. When a laser field is very broadband the chromatic nature of diffraction becomes relevant, affecting both the pulse amplitude and phase through the focus [16]. The effect has been measured on-axis and off-axis for linearly polarized pulses using a variety of techniques [19–22], and can be conceptualized by comparing two distinct physical scenarios of laser beam production and focusing, shown in Fig. 1.

If a laser beam is synthesized in such a way that on the collimated beam all frequencies have the same beam

waist W_i and a Gaussian spatial profile, when focused with a perfect focusing element having focal length f each frequency will have a beam size $w_0(\omega) = \frac{2cf}{\omega W_i}$ in the focus (see Fig. 1(a)). This matters because the in-focus field is generally the relevant field for simulations or experiments. In contrast, if a laser beam is synthesized in way such that all frequencies have the same waist w_{00} , and then collected, the collimated beam will have the waist $W_0(\omega) = \frac{2cf}{\omega w_{00}}$. In this second case when the large collimated beam is re-focused, the waist will be constant again in the experimental focus (see Fig. 1(b)).

As an even further complication, the Rayleigh range is not constant in either of these two cases since $z_R = \frac{\omega w_0^2(\omega)}{2c}$ depends on frequency. This underscores the lack of validity of the common model of pulse focusing, which usually operates on the approximation that both the beam waist and Rayleigh range are frequency-independent quantities related to the central frequency. As the pulse duration decreases (bandwidth increases) the common approximation becomes less accurate. In this work we show that in vacuum acceleration simulations with few-cycle RPLBs it is crucial to consider the correct model of frequency-dependence of the beam parameters corresponding to the physical scenario in question, whatever it may be.

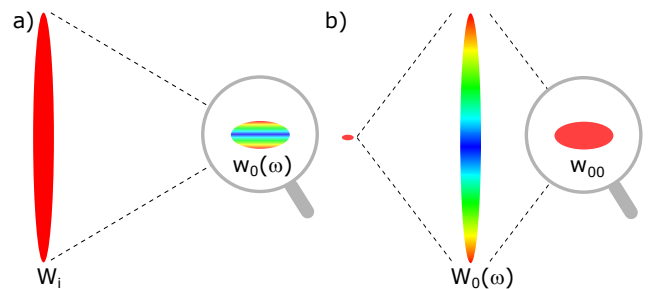


FIG. 1. Two examples of unique physical scenarios that require different descriptions in the focus in order to properly model the field. In (a) the collimated beam has a constant beam size, but in-focus the beam size depends on frequency. In (b) it is reversed.

* spencer.jolly@cea.fr

The relationships between the beam waist and Rayleigh range on the input beam, W_0 and Z_R respectively, and on the focused beam, w_0 and z_R respectively, are as follows: $Z_R = \frac{\omega W_0^2}{2c}$, $z_R = \frac{\omega w_0^2}{2c}$, and $w_0 = \frac{2cf}{\omega W_0}$. Any one parameter of W_0 , Z_R , w_0 , z_R may depend arbitrarily on frequency, but the relationships are fixed by diffraction theory. This is crucial for understanding the various situations presented throughout the rest of this manuscript.

The two physical scenarios shown in Fig. 1 are differentiated by the frequency-dependent beam waist of collimated input beam. But in fact, such situations can be classified by a single parameter g_0 referred to as the "Porras factor" [16, 22]

$$g_0 = \left. \frac{dZ_R(\omega)}{d\omega} \right|_{\omega_0} \frac{\omega_0}{Z_R(\omega_0)}. \quad (1)$$

With this new factor in mind we can refer to the different scenarios more easily. The case where the input beam size W_0 is constant corresponds to $g_0 = 1$, which also is a case where the beam is iso-diffracting in the focus (i.e. w_0/z_R is constant), and is the same as Fig. 1(a). The case where the focused beam size w_0 is constant corresponds to $g_0 = -1$, where the input beam is iso-diffracting (i.e. W_0/Z_R is constant), and is the same as Fig. 1(b). A third case $g_0 = 0$ is where the Rayleigh ranges both on the input beam and the focused beam are frequency-independent ($Z_R = f^2/z_{R0}$). Keep in mind that none of these cases correspond to the simplification that both the beam waist and Rayleigh range are frequency-independent.

More generally, if we define $w_0(\omega_0) = w_{00}$ as the reference value, since we often model the interaction in the focal region and the beam size is easiest to measure, this results in $z_R(\omega) = (\omega_0 w_{00}^2 / 2c)(\omega_0/\omega)^{g_0}$ and $w_0(\omega) = w_{00}(\omega_0/\omega)^{\frac{g_0+1}{2}}$. Complete descriptions of the phase at arbitrary longitudinal and transverse locations throughout the focal volume have been derived for linearly polarized light [16, 23, 24], but we will consider rather the longitudinal field produced from focusing radially-polarized Gaussian light fields for the acceleration application.

We will first study only on-axis acceleration with RPLBs, where the electron is constrained to a trajectory only on $r = 0$ where the purely E_z field is responsible for acceleration. Then we will look at off-axis acceleration as well, where the fully frequency-dependent model becomes even more important. For all simulations we will use a focused beam waist defined at the central frequency as $w_0(\omega_0) = w_{00} = 4 \mu\text{m}$ and calculate the Rayleigh range and beam waist at different frequencies corresponding to the g_0 value under consideration. All simulations will be done with pulses having a central wavelength λ_0 of 800 nm ($\omega_0 = 2\pi\lambda_0/c$).

The on-axis longitudinal electric field in frequency space is modelled within the paraxial approximation according to past work [12]

$$\hat{E}_z(z, \omega) = \sqrt{\frac{8P_0}{\pi\epsilon_0 c}} \frac{A(\omega)}{z_R(\omega) \left(1 + \left(\frac{z}{z_R(\omega)}\right)^2\right)} e^{i\psi(z, \omega)} \quad (2)$$

$$\psi(z, \omega) = \Psi_0 + 2 \tan^{-1} \left(\frac{z}{z_R(\omega)} \right) - \frac{\omega z}{c}, \quad (3)$$

where $A(\omega)$ is the integrated frequency content of the pulse, $z_R(\omega)$ is the in-focus Rayleigh range, P_0 is the beam power, Ψ_0 is the constant CEP offset phase, and ϵ_0 and c are physical constants. The modeling in frequency space is necessary because when z_R depends on frequency, which we have shown to be necessary to properly describe commonly existing scenarios, the field in time is not simple to describe and will have a modified amplitude and phase compared to the frequency-independent case. The paraxial approximation which produces Eqs. (2)–(3) is only valid for the on-axis acceleration that we present first [6].

The electric field in time, calculated via the Fourier transform, is necessary to simulate the electron acceleration via the relativistic Lorentz force and a 5th-order Adams-Bashforth finite-difference method as in much past work [3, 12]. The simulations start at a large enough negative time such that the pulse is not influencing the electron and they continue until the pulse has completely overtaken the particle and the kinetic energy is no longer changing significantly. We study the final kinetic energy of electrons initially at rest for a range of laser powers, pulse durations, and g_0 values, optimized over the initial position $z(0)$ of the electron and the CEP phase Ψ_0 of the laser pulse.

We first look at laser pulses that have a Gaussian spectrum with characteristic $1/e^2$ spectral width $\Delta\omega$ and pulse duration $\tau_0 = 2/\Delta\omega$. Using these Gaussian pulses we study acceleration with laser pulses having durations of 15 and 7.5 fs up to powers of 300 TW, comparing the default scenario of a constant z_{R0} ($g_0 = 0$) to that with $g_0 = 1$. We choose $g_0 = 1$ since it corresponds to the scenario in Fig. 1(a), which we consider to be a very likely scenario for lasers having these power levels. We extend this analysis to laser pulses of 3.5 fs duration that have a Poisson-like spectrum, which is necessary to properly model the pulse according to Maxwell's equations as the pulse approaches the few-cycle regime [15]. The results are shown in Fig. 2(a).

The key conclusions of the results presented in Fig. 2(a) are that the $g_0 = 1$ scenario decreases the final kinetic energy in all cases relative to the $g_0 = 0$ case, and that the relative decrease becomes more severe as the pulse duration decreases. At 130 TW power in the case of 3.5 fs duration the decrease is by 75 %, where with 15 fs duration the decrease is only by 13 %. For all durations this decrease becomes less severe as the laser power increases. At 300 TW the decrease is 16 % and 4.5 % for 3.5 fs and 15 fs respectively.

We also consider acceleration with beams having a larger set of g_0 values for the shortest pulse duration of

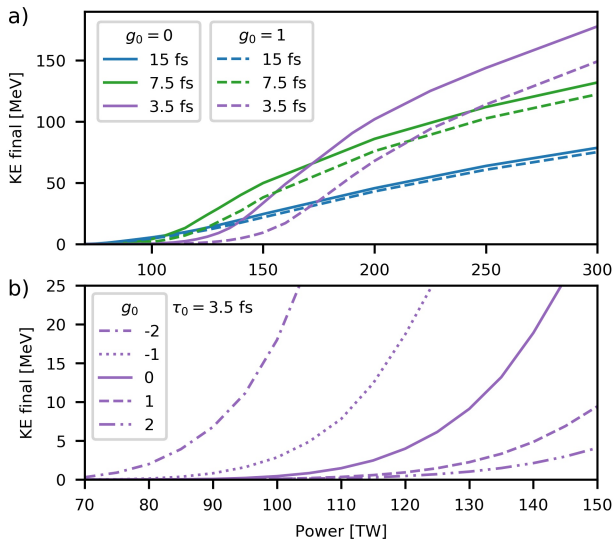


FIG. 2. (a) Summary of on-axis results at durations of 15, 7.5, and 3.5 fs with the constant z_{R0} ($g_0 = 0$) assumption (solid lines) and with $g_0 = 1$ (dashed lines). (b) On-axis results at a duration of 3.5 fs for a variety of g_0 values.

3.5 fs, with the results shown in Fig. 2(b). We include the results already presented at $g_0 = 0$ and 1 for this duration, and expand to include -2, -1, and 2 in the range of laser powers from 70–150 TW. The surprising results are that, where the $g_0 = 1$ case produced a lower final kinetic energy, the cases of negative g_0 produce a higher final kinetic energy, increasing as g_0 becomes more negative. When $g_0 = 2$ the final kinetic energy is massively decreased.

The explanation for this drastic difference in the final kinetic energy must be related to the change in the Gouy phase and central frequency within the focal area for different g_0 values, as derived in Ref. [23] and measured in Ref. [22] for linearly-polarized pulses. We numerically calculate the CEP and central frequency change through the focus for the on-axis E_z field of the focused radially-polarized pulses, with the results shown in Fig. 3(a)–(b). The Gouy phase results notably show a similar behavior as in the previous work with linear polarization, i.e. increasing steepness as g_0 becomes negative and an inflection as g_0 become positive, but with a total shift of 2π . This 2π shift conflicts with previous work on the Gouy phase in highly non-paraxial focusing [25–27], where they observed only a shift of π , but since we are in the paraxial regime this is to be expected.

The impact of the combination of the slightly modified spatio-spectral amplitude and the Gouy phase is that the field at a given time and position is different for the various g_0 values, impacting the acceleration as the electron slips behind the laser pulse. We demonstrate this by looking at three acceleration trajectories for g_0 values of 1, 0, and -1 at 125 TW shown in Fig. 3(c). Each case has its own optimum constant offset phase

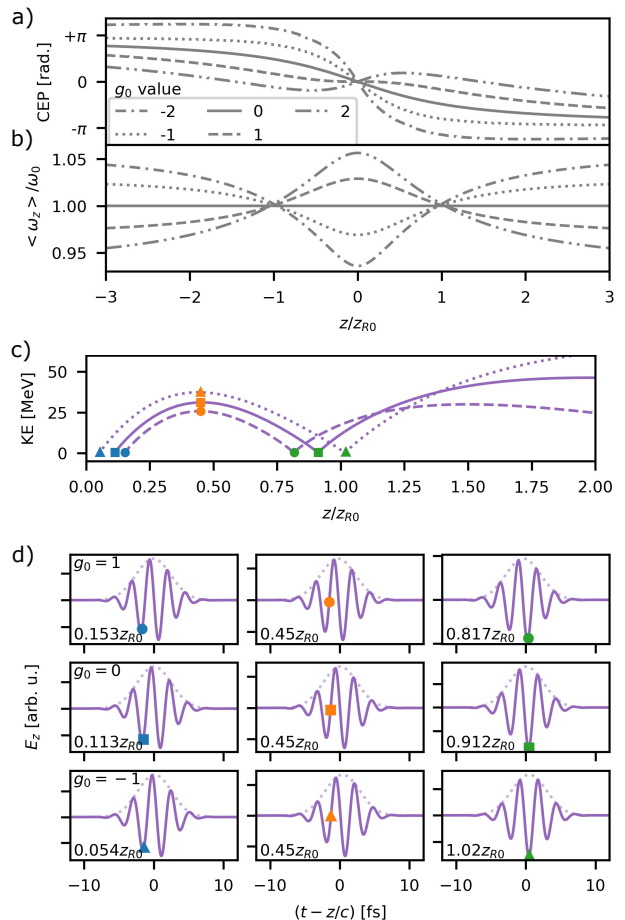


FIG. 3. The Gouy phase behavior (a) and the central frequency ω_z (b) of E_z on-axis depend strongly on the g_0 value. Three trajectories at 125 TW (c) show the different nature of the acceleration (each case having a different optimum $z(0)$). Snapshots of the field (d), with the location of the electron shown with the symbols (circles, squares, triangles), in each case having a different optimum constant Ψ_0 , show the case of $g_0 = -1$ having the best CEP at the start of the final accelerating half-cycle, resulting in more acceleration. The positions of the snapshots in (d) are shown in (c) with the corresponding symbols and colors.

Ψ_0 and initial electron position $z(0)$. Taking snapshots of the field at the points in each case where the accelerating field is strongest in the second-to-last accelerating half-cycle (left column of Fig. 3(d)), where the field switches from accelerating to decelerating (middle column of Fig. 3(d)), and where the field is strongest in the last accelerating half-cycle (right column of Fig. 3(d)) explains the difference in acceleration. The CEP for the case of $g_0 = -1$ in the lower row of Fig. 3(d) is such that the decelerating field is below the maximum that it could be when the electron enters the decelerating half-cycle, and when the electron enters the final accelerating half-cycle the CEP has evolved such that the field is at its maximum possible. The opposite is for the case of

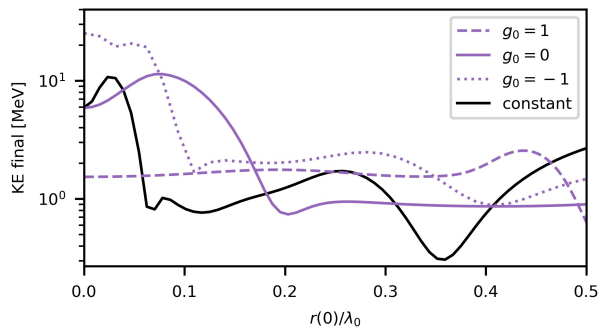


FIG. 4. The results of off-axis simulations with varying initial radial position $r(0)$ show a stark difference between cases of varying g_0 , but also a lack of agreement between $g_0 = 0$ and the common approximation of constant parameters. Initial electron position $z(0)$ and laser CEP are optimized for the on-axis final energy, and are therefore the same as in Fig. 2(b) for 125 TW.

$g_0 = 1$ in the upper row of Fig. 3(d), resulting in less acceleration. The evidence in Fig. 3(d) shows that the different CEP evolution shown in Fig. 3(a) results in a more favorable situation when g_0 is negative.

The analysis of on-axis acceleration was instructive and clearly showed that as the pulse duration decreases, proper modeling becomes crucial. The same discussion of including the frequency-dependence of the beam parameters is important for off-axis simulations as well, but there is another dimension that becomes relevant. Where the on-axis field in Eqs. (2)–(3) only included the Rayleigh range, the off-axis field equations include independently the beam waist and the Rayleigh range [4]. Therefore the off-axis field equations in the frequency-independent approximation are lacking the proper form for either the beam waist or the Rayleigh range (since they cannot both be frequency-independent, as discussed earlier), and therefore do not correspond exactly to any physical scenario regardless of the g_0 value.

The model for off-axis acceleration is an extension of the model already used on-axis in Eqs. (2)–(3). The off-axis fields including E_r and B_θ must be included along with the non-paraxial terms [6]. We implement this using the fields derived in Ref. [4] in the frequency domain, which are expanded in terms of the small parameter $\epsilon = w_0/z_R$ that can now depend on frequency. We Fourier-

transform the fields to time and calculate the force on the particles as before. We again use a constant beam waist at the central frequency $w_0(\omega_0) = w_{00} = 4 \mu\text{m}$ and vary the g_0 value, but to limit the parameter space we simulate a laser pulse with a duration of 3.5 fs, a power of 125 TW, and a CEP optimal according to the on-axis accelerated energy (i.e. the same CEP as Fig. 3(d)). We simulate the electron trajectories having begun at different off-axis positions $r(0)$, but always with the same initial longitudinal position (i.e. the same $z(0)$ as Fig. 3(c)). We also compare the properly modelled results with varying g_0 to the fully frequency-independent situation (which is not physically correct), where both w_0 and z_R are constant values related to the central frequency.

The off-axis simulation results are shown in Fig. 4. It is clear that the results in the different g_0 scenarios are also very different off-axis, meaning that the proper modeling is important for the entire process, and not just on-axis trajectories. However, the most important result may be that there is significant difference between the $g_0 = 0$ case and the results using the frequency-independent approximation. This means that regardless of the g_0 value under consideration the frequency-dependent model is necessary to produce correct results for all trajectories. The impact of the differences becomes more significant especially for applications aiming for electron beams with designed charge or emittance values, since the effect on the off-axis trajectories is not straightforward.

In conclusion, we have shown that simulating electron acceleration with few-cycle radially-polarized laser fields requires proper modeling of the spatio-spectral amplitude described in this case by the g_0 value. This is not only detrimental in the commonly occurring case of $g_0 = 1$, providing a strong motivation for characterizing experimental driving pulses with spatio-spectral characterization devices [28], but could be a path toward optimizing the acceleration process with shaped amplitude profiles having negative g_0 , or having a more complex shape that cannot be described by a single parameter. We have shown that these dynamics are due to the varying CEP evolution through the focus in the different cases, and that this need for proper modeling applies to both on-axis and off-axis trajectories. The implications of these results may extend to other areas of very broadband field-sensitive laser-matter interactions such as photoelectron production, high-harmonic generation, and the interaction of intense laser-pulses with solid-density plasmas.

-
- [1] C. Varin, M. Piché, and M. A. Porras. Acceleration of electrons from rest to GeV energies by ultrashort transverse magnetic laser pulses in free space. *Physical review E*, 71:026603, 2005.
- [2] P.-L. Fortin, M. Piché, and C. Varin. Direct-field electron acceleration with ultrafast radially polarized laser beams: scaling laws and optimization. *Journal of Physics B: Atomic, Molecular and Optical Physics*, 43:025401, 2010.

- [3] L. J. Wong and F. X. Kärtner. Direct acceleration of an electron in infinite vacuum by a pulsed radially-polarized laser beam. *Optics Express*, 18(24):25035–25051, 2010.
- [4] Y. I. Salamin. Fields of a radially polarized Gaussian laser beam beyond the paraxial approximation. *Optics Letters*, 31(17):2619–2621, 2006.

- [5] V. Marceau, A. April, and M. Piché. Electron acceleration driven by ultrashort and nonparaxial radially polarized laser pulses. *Optics Letters*, 37(13):2442–2444, 2012.
- [6] V. Marceau, C. Varin, and M. Piché. Validity of the paraxial approximation for electron acceleration with radially polarized laser beams. *Optics Letters*, 38(6):821–823, 2013.
- [7] V. Marceau, C. Varin, T. Brabec, and M. Piché. Femtosecond 240-keV electron pulses from direct laser acceleration in a low-density gas. *Physical Review Letters*, 111:224801, 2013.
- [8] A. Martens, K. Dupraz, K. Cassou, N. Delerue, A. Variola, and F. Zomer. Direct electron acceleration with tightly focused $TM_{0,1}$ beams: boundary conditions and non-paraxial corrections. *Optics Letters*, 39(4):981–984, 2014.
- [9] L. J. Wong, K.-H. Hong, S. Carbajo, A. Fallahi, P. Piot, M. Soljačić, J.D. Joannopoulos, F. X. Kärtner, and I. Kaminer. Laser-induced linear-field particle acceleration in free space. *Scientific Reports*, 7:11159, 2017.
- [10] S. Payeur, S. Fourmaux, B. E. Schmidt, J. P. MacLean, C. Tchervakov, F. Légaré, M. Piché, and J. C. Kieffer. Generation of a beam of fast electrons by tightly focusing a radially polarized ultrashort laser pulse. *Applied Physics Letters*, 101:041105, 2012.
- [11] S. Carbajo, E. A. Nanni, L. J. Wong, G. Moriena, P. D. Keathley, G. Laurent, R. J. D. Miller, and F. X. Kärtner. Direct longitudinal laser acceleration of electrons in free space. *Physical Review Accelerators and Beams*, 19:021303, 2016.
- [12] S. W. Jolly. Influence of longitudinal chromatism on vacuum acceleration by intense radially polarized laser beams. *Optics Letters*, 44(7):1833–1836, 2019.
- [13] M. A. Porras. Ultrashort pulsed gaussian light beams. *Physical Review E*, 58(1):1086–1093, 1998.
- [14] S. Feng, H. G. Winful, and R. W. Hellwarth. Gouy shift and temporal reshaping of focused single-cycle electromagnetic pulses. *Optics Letters*, 23(5):385–387, 1998.
- [15] C. F. R. Caron and R. M. Potvliege. Free-space propagation of ultrashort pulses: Space-time couplings in gaussian pulse beams. *Journal of Modern Optics*, 46(13):1881–1891, 1999.
- [16] M. A. Porras. Diffraction effects in few-cycle optical pulses. *Physical Review E*, 65:026606, 2002.
- [17] X.-M. Cai, J.-Y. Zhao, Q. Lin, and J.-L. Luo. Electron acceleration by subcycle pulsed focused vector beams. *Journal of the Optical Society of America B*, 33(2):158–164, 2016.
- [18] X. Cai, J. Zhao, Q. Lin, H. Tong, and J. Liu. Electron acceleration driven by sub-cycle and single-cycle focused optical pulse with radially polarized electromagnetic field. *Optics Express*, 26(23):30030–30041, 2018.
- [19] F. Lindner, G. G. Paulus, H. Walther, A. Baltuška, E. Goulielmakis, M. Lezius, and F. Krausz. Gouy phase shift for few-cycle laser pulses. *Physical Review Letters*, 92(11):113001, 2004.
- [20] T. Tritschler, K. D. Hof, M. W. Klein, and M. Wegener. Variation of the carrier-envelope phase of few-cycle laser pulses owing to the gouy phase: a solid-state-based measurement. *Optics Letters*, 30(7):753–755, 2005.
- [21] B. Major, D. Nemes, M. A. Porras, Z. L. Horváth, and A. P. Kovács. Carrier-envelope phase changes in the focal region: propagation effects measured by spectral interferometry. *Applied Optics*, 54(36):10717–10724, 2015.
- [22] D. Hoff, M. Krüger, L. Maisenbacher, A. M. Saylor, G. G. Paulus, and P. Hommelhoff. Tracing the phase of focused broadband laser pulses. *Nature Physics*, 13:947–952, 2017.
- [23] M. A. Porras. Characterization of the electric field of focused pulsed gaussian beams for phase-sensitive interactions with matter. *Optics Letters*, 34(10):1546–1548, 2009.
- [24] M. A. Porras, Z. L. Horváth, and B. Major. Three-dimensional carrier-envelope-phase map of focused few-cycle pulsed gaussian beams. *Physical Review A*, 98:063819, 2018.
- [25] X. Pang and T. D. Visser. Manifestation of the Gouy phase in strongly focused, radially polarized beams. *Optics Express*, 21(7):8331–8341, 2013.
- [26] K. J. Kaltenecker, J. C. König-Otto, M. Mittendorff, S. Winnerl, H. Schneider, M. Helm, H. Helm, M. Walther, and B. M. Fischer. Gouy phase shift of a tightly focused, radially polarized beam. *Optica*, 3(1):35–41, 2016.
- [27] A. Woldegeorgis, T. Kurihara, M. Almassarani, B. Beleites, R. Grosse, F. Ronneberger, and A. Gopal. Multi-MV/cm longitudinally polarized terahertz pulses from laserthin foil interaction. *Optica*, 5(11):1474–1477, 2018.
- [28] C. Dorrer. Spatiotemporal metrology of broadband optical pulses. *IEEE Journal of Selected Topics in Quantum Electronics*, 25(4):3100216, 2019.